

# The Coupled Logistic Map and Covid Dynamics

Ruchina Shakya  
Dept. of Computer Science  
University of New Mexico  
rshakya@unm.edu

Nicholas Bacon  
Dept. of Computer Science  
University of New Mexico  
Nbacon@unm.edu

Yingfan Wang  
Dept. of Computer Science  
University of New Mexico  
yingfan3@unm.edu

**Abstract**—The unexpected degree of complexity is determined through a logistic map. In this project, we extend the idea of transition from bottom-up to top-down causation with comprehensive analysis utilizing logistic maps. We used Shannon entropy and mutual information to measure the average amount of information needed to describe the outcomes of distribution and transfer entropy to measure the causality.

## I. INTRODUCTION

A logistic map is a one-dimensional discrete-time map to examine the behavior. It explains the flow of structure and the dynamics. Predicting if the population will grow or shrink over time. The initial/starting two trajectories in the logistic map might look similar and close off at first but diverge with increasing time. This is called a chaotic system. It is referred to as sensitive dependence on initial conditions. The chaotic behavior appears in the lowest dimension. Therefore, it uses the logistic map. Transfer entropy explains the deviation from the expected entropy of two completely independent processes[1]. TE depends on the past values of the variables. The equation for the transfer entropy for two completely independent processes (X and Y) is:

$$T_Y^{(k)} \rightarrow X = \frac{p(x_{n+1}, x_n^{(k)}, y_n^{(k)}) \log \frac{p(x_{n+1}|x_n^{(k)}, y_n^{(k)})}{p(x_{n+1}|x_n^{(k)})}}{p(x_{n+1}, x_n^{(k)})} \quad (k) \quad (k)$$

where  $x_n^{(k)}$  and  $y_n^{(k)}$  are delayed states to the  $x_{n+1}$ .  $k$  is the embedding dimension.  $T_Y^{(k)} \rightarrow X$  measures the information flow from Y to X. The calculation of difference in transfer entropy between  $T_X^{(k)} \rightarrow Y$  and  $T_Y^{(k)} \rightarrow X$  determines the dominant information flow.

The main purpose of the paper is to provide insight on the top-down causation. It states that the driving force for most major evolutionary transitions comes from the reversal in the flow of information from lower to higher levels to that from higher to lower levels. It focuses on the new higher-level entities produced by the evolutionary transitions. The new higher-level entities produced are the outcome of the units which used to reproduce without any external control. The methods used in Walker's paper that we used for analysis are Shannon entropy, mutual information, and transfer entropy. The mutual information method helped to visualize the joint probability of two processes.

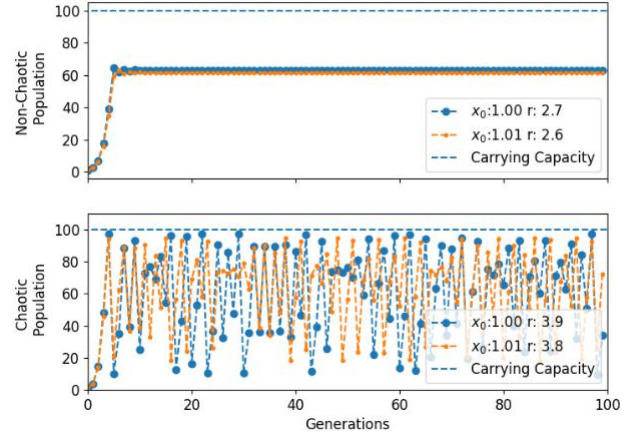


Fig. 1. Time series of non-chaotic(top,  $r = 2.7, 2.6$ ) and chaotic population(bottom,  $r = 3.9, 3.8$ ) with two different reproductive coefficient in each.

The major reason to use a logistic map is to analyze the increase and decrease of Covid infection over some time with different growth rates. The logistic map gave a strong picture of the Covid infection growth rate in three different states(Nebraska, Iowa, South Dakota). The concept of transition from bottom-up to top-down causation was used to detect the influence on Covid dynamics.

## II. METHODS AND RESULTS

### A. Shannon Entropy and Mutual Information

The figure demonstrates the Shannon entropy and the mutual information in chaotic and non-chaotic time series. In [fig. 1], two sets of two-time series were taken with the different growth rates in each. The two reproduction coefficients picked for the non-chaotic series are ( $r = 2.7$  and  $r = 2.6$ ) and for chaotic series are ( $r = 3.9$  and  $r = 3.8$ ). The coefficients were selected to represent both chaotic and non-chaotic behavior. The initial population was varied by 1% of the other for both of the behaviors( $x_0 = 1.00, 1.01$ ). The carrying capacity is the same for both time series. The coefficient of the non-chaotic series is less than the chaotic threshold therefore, it eventually reaches an equilibrium state. From [fig. 1] we can see that after passing a few generations, the synchronization occurs in the non-chaotic series reaching an equilibrium state. The chaotic

series from [fig.1] stays together for the first 15 generations and starts diverging after with no signs of synchronization. In [fig. 2], the four Venn diagram shows the Shannon entropy( $H(X), H(Y)$ ) and mutual information( $I(X,Y)$ )[2]. The first 15 generations and last 15 generations were taken to find the Shannon entropy and mutual information. The overlapping in the diagram shows the mutual information and the non-overlapping individual part in the circle shows the entropy. The measurement of these was done using the JIDT tool using a binned method of measurement(15 bins). The first 15 non-chaotic[fig. 2] shows the mutual information(1.375279 bits) overlap. However, there is a presence of entropy as mutual information does not completely overlap. We can observe this from [fig. 1] as well. In the first 15 chaotic series[fig. 2], there is a presence of closely identical entropy measures(3.3232314 bits and 3.506891 bits).

The entropy starts growing in both individuals as the generation increases with time. There would not be an overlap as the individuals start diverging. The mutual information(1.252530 bits) is close to half of the individual entropy of the first 15 chaotic diagrams. In the first 15 non-chaotic series, the value of both individuals meets at the same point. Therefore, leading entropy measure and mutual information to a zero value. The diagram does not exist for this relation. The last 15 chaotic diagram, it is observed to be similar to the first 15 chaotic diagram with similar mutual information(1.096649 bits). The transfer entropy for each of the chaotic and non-chaotic, first and last (15generations) with  $k=2$  was calculated. The transfer entropy in the first and last non-chaotic was found to be 0. This means it reaches the synchronization point. The transfer entropy for the first and last 15 generations chaotic behavior measures 0.1238 bits and 0.1896bits respectively.

## B. Replication of Walker's Toy Model

The Walker paper uses logistic growth as a toy model as it has a strong connection with the replicative growth of biological populations. It mainly focuses on a lattice of chaotic logistic maps to explore non-trivial collective behavior and its connection to transitions in causal structure. A model system is defined with the current time-step( $n$ ).

$$x_{i,n+1} = (1 - \epsilon)f_i(x_{i,n}) + \epsilon m_n ; (i = 1, 2, \dots, N) \quad (2)$$

In this equation,  $N$  is the total number of elements. The  $\epsilon$  is the global coupling strength to the mean population. It is indicative of the variations in the degree influenced by dynamics of mean-field and individual local elements.

$$f_i(x_{i,n}) = r_i x_{i,n} \left(1 - \frac{x_{i,n}}{K}\right) \quad (3)$$

The  $f_i(x_{i,n})$  represents the local dynamics of element  $i$  where  $r_i$  is the reproductive fitness of population  $i$ . The carrying capacity( $K$ ) which is the maximum population size is 100.

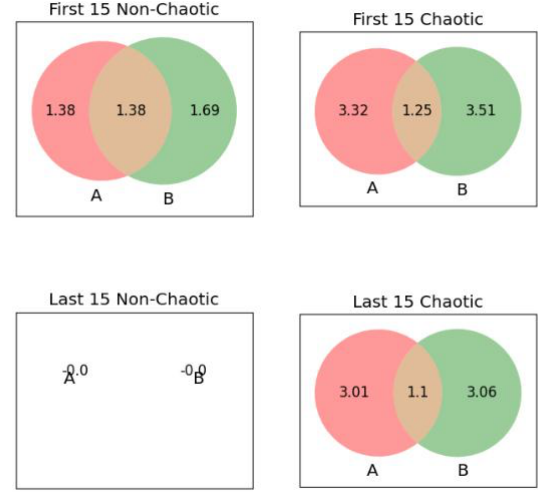


Fig. 2. Venn diagrams illustrating the relative scale of the entropies and mutual information. The data was collected from Fig. 1. Logic map. Note: On the Last 15 Non-Chaotic Venn diagram the entropies of both sets are 0 therefore the circle has an area of 0.0.

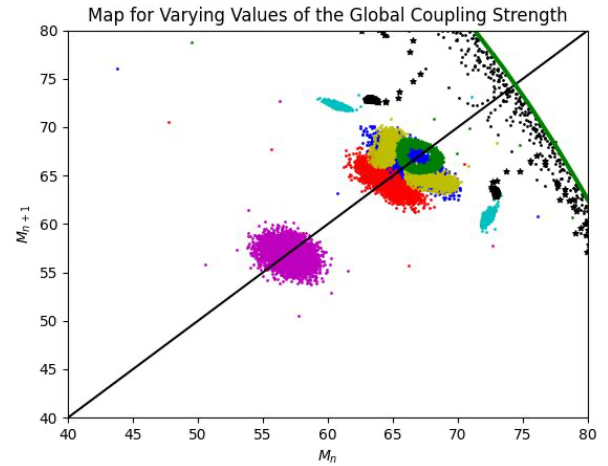


Fig. 3. Return map for different values of global coupling strength  $\epsilon$ . The figure shows the return maps for  $\epsilon = 0$  (magenta),  $\epsilon = 0.075$  (red),  $\epsilon = 0.1$  (blue),  $\epsilon = 0.2$  (yellow),  $\epsilon = 0.225$  (cyan),  $\epsilon = 0.25$  (dark green),  $\epsilon = 0.3$  (stars), and  $\epsilon = 0.4$  (black). The borderline on the top corner (green) is the single logistic map.

$M_n$  is the instantaneous mean-field calculated by the average of the local population.

$$M_n = \frac{1}{N} \sum_{j=1}^N x_{j,n} \quad (4)$$

The instantaneous dynamics of the mean field is calculated by the average of  $f_j(x_{j,n})$  for all populations. The equation for  $M_n$  is shown below: It is also known as the instantaneous state of meta-population. The equation for instantaneous dynamics of the mean field is shown below:

$$m_n = \frac{1}{N} \sum_{j=1}^N f_j(x_{j,n}) \quad (5)$$

It is a global entity that impacts the dynamics of local elements in the model system. The local attribute does not play any part in this equation.

We used the same values as Walker's paper to represent the toy model. [Fig. 3] displays different phases with dynamical properties. It was initialized with  $x_{i,0} = 1$  which represents an initial population size. A set of  $N = 1000$  coupled logistic maps were recorded for 10000 generations. The fitness parameter  $\text{range}(r_i)$  was in-between  $[3.9, 4.0]$ . According to the Walker paper, this range was strictly chosen to show chaotic dynamics even when coupled to the global dynamics. Time series of  $(x_i, n)$  and  $M_n$  were generated and recorded. The series helped us define the direction of cause and the associated flow of information. When the  $\epsilon = 0$ , there is no global coupling. There is no influence on individuals. The maximum epsilon value i.e 1 leads to complete coupling. In [Fig.3], all the values were set up to run a return map with different global coupling strengths ( $\epsilon$ ). The graph represents the global population of time  $n$  and the global population of time  $n + 1$ . We can see in [Fig.3], the magenta color shows a cloud-like point in the middle because of the absence of global coupling(0). There is no structure or pattern to see what happens next. The small amount of change in  $\epsilon(0.075)$  leads to a quite higher point with some global coupling. But we did not observe the same pattern as the Walker paper. Epsilons with a global coupling are found bouncing back and forth( $\epsilon = 0.225$ ) in very distinct regions(red cluster with other color clusters with some points flying around) in the global population. The multiple colors(red, blue, yellow) clusters were observed to be compact with each other in the return map above average. The multiple clouds have been observed to have similar behaviors showing high top-down information transfer. The two black stars( $\epsilon = 0.3$ ) in the graph represent the big enough  $\epsilon$  which forms a steady global population that stays in sync. The  $\epsilon$  with the high value( $\epsilon = 0.4$ (black)) has the highest influence in the individual local population with chaotic behavior. From the return map, we observe multiple clusters showing high top-down information flow resulting in the emergence of collective behavior[1]. The results are further passed to top-down and bottom-up transfer entropy to reflect collective dynamics.

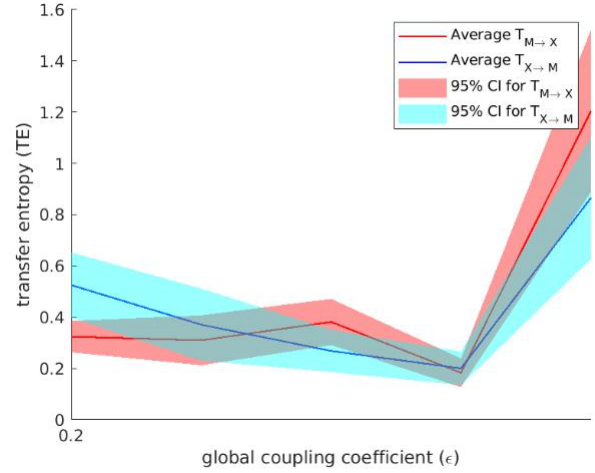


Fig. 4. A zoomed of 0.2 to 0.3 in picture of the Mean and 95% confidence in-intervals (CI) of top-down(red) and bottom-up(blue) causal information transfer. This graphic is displayed as a function of global coupling straight  $\epsilon$

### C. Information Transfer: Evaluating Bottom-Up and Top-Down Perspectives

Transfer entropy measures the information flow from bottom-up to top-down. The transition probability is required to work out causal information transfer. Walker's paper uses Markov's process of ordering  $k$ . It uses  $x^{(k)}_n$  which contains all the necessary information to characterize the trajectory of the dynamical variable  $x$ .  $x^{(k)}_n = (x_n, \dots, x_{n-k+1})$  is a embedded state. Therefore, it introduces the transfer entropy equation[5] which measures causal relationships by connecting the lag states  $(x^{(k)}_n, y^{(k)}_n)$  to  $x_{n+1}$  state. It is measured in bits. The  $k$  value is the dimension of embedding.  $T_{Y \rightarrow X} = \text{Max}(T_{Y^{(k)} \rightarrow X})$ .

$$T_{Y \rightarrow X}^{(k)} = p(x_{n+1} | X_n^{(k)}, Y_n^{(k)}) \quad (6)$$

The flow of information from local to global scales ( $T_{X \rightarrow M}$ ) and from global to local scales ( $T_{M \rightarrow X}$ ) was compared to study the causal information transfer from the global to the local dynamics and how it corresponds to the emergence of collective organization.

The transfer entropy was calculated using the JIDT tool which later on generated MatLab code. We use the same approach as the paper from 2020 by Deterding and Wright[2]. To calculate the entropy we took the  $k$  values 1 and 2. The carrying capacity( $K$ ) and the initial population are the same as the toy model approach. We simulated 10 metapopulations with each containing 1000 sub-populations which simulated over 1000 generations. The data points were collected. The three  $\epsilon$  values picked are 0.225, 0.250, 0.275. We were unable to use the  $k$  values 3 and 4 to calculate the entropy because of the same error in Deterding and Wright paper. [Fig.4] shows the top-down casual information transfer in red and bottom-up transfer in light blue with the 95% confidence bands around

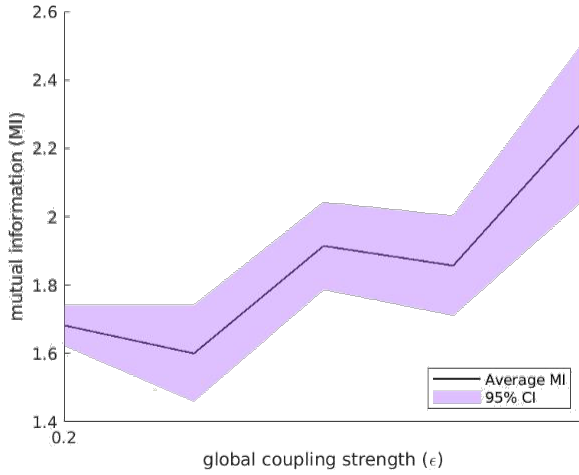


Fig. 5. A zoomed of 0.2 to 0.3 in the picture of the Average mutual information(MI) measured in bits between sub-populations. A 95% confidence interval is showing the uncertainty in the MI

each information with its respective colors. After zooming into the global coupling coefficient(0.2) in [Fig.4], we can observe a top-down dominance. We can see the information transfer flow because we stretched into the global coupling value of 0.2 moving towards 0.3. This shows the uncertainty between 0.2 and 0.3( $0.2 \leq \epsilon < 0.3$ ). It is difficult to determine which direction has the highest flow of energy. But, looking into [fig. 3], we can determine  $\epsilon = 0.3$  is moving towards the periodic line. The mean-field starts a chaotic behavior when the epsilon value is moved to 0.4. Therefore, the top-down information flow dominated the bottom-up when  $\epsilon > 0.3$ . [fig. 5] shows the measure of mutual information to global coupling strength with the 95% of confidence bands. We calculated the mutual information of sub-population present in the 10 meta-populations using the JIDT tool. Each meta population produced 3 data points for the subpopulations. The minimum point observed in [fig.5] shows information flow change from bottom-up to top-down. We did not observe a clear quasi-periodic three-state oscillatory dynamic as Walker's paper in [fig.3] when  $\epsilon = 0.075$ . But, we did observe two-phase periodic oscillation when  $\epsilon = 0.225$ . This indicates top-down information transfer does not depend on the three-state oscillatory dynamics as Walker's paper defined.

#### D. Apply methods to the real world the Coronavirus Data

For this part, we chose Nebraska, Iowa, and South Dakota. We picked these states since they share borders, use similar measures to respond to Covid like laws, lockdown, and social distance. The populations of these 3 states are politically similar and they have similar vaccination rates. As of Feb 18 the full vaccination rate of Iowa – 60.9%, Nebraska – 62.3%, and South Dakota is 59.6%.[6] We found a data set of daily Covid cases per 100k in these states from 1/1/2020 to 2/1/2022 and took the log of the data showing in [fig.6]. We chose to manipulate the data and calculate the Shannon Entropy(SE)

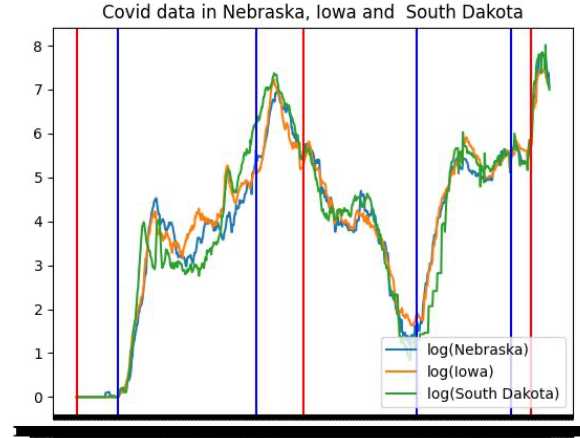


Fig. 6. This is real-world Covid data from the New York Times. We applied a log to the data to raise the Mutual information and Entropy. The red lines indicate 01/01/2020,01/01/2021 and 01/01/2022, blue lines indicate key dates we will mention later

States	NE	IA	SD
Entropy	0.233150	0.343002	0.318419
States Pair	IA&NE	SD&IA	SD&NE
Mutual Information	1.741240	1.514749	1.464189

Fig. 7. Total Entropy and Mutual

and the Mutual Information(MI) of the total set. We have calculated the SE and MI of data without any manipulations, with a log normalization and then smoothing data respectively. For the smoothing, we used DCT and only kept 10% low frequencies. We found that both MI and SE were higher after log normalization but went down after smoothing. Therefore, we decided to forego smoothing the data for the next parts and we put the data without smoothing in the table.

The results are shown as [fig.6]. We chose four key dates(where the blue lines are) and the 2 months after them in this graph. The first key date, 03/08/2020; this is the day that lockdown and restriction started. The second key date, 10/17/2020; this is the day that the government started recommending people to wear masks indoors and in crowded areas. Next key day, 07/01/2021; this is the day that 50% of people got fully vaccinated. Lastly is the fourth key date, 12/01/2022; this is the day the first Omicron case was found in the USA. To compare them we calculated MI among three states. MI indicates the correlation between two random variables. The higher the MI is, the higher correlation they have. In other words, the uncertainty of using one variable to predict the other is also lower. That's why we think that MI is a piece of strong evidence to test if the hypothesis is correct. In this case, MI shows the correlation of trending among Covid cases. The results are shown as [fig.7] (from key dates to two months later is a process ).

Take the first graph as an example, every circle rep-



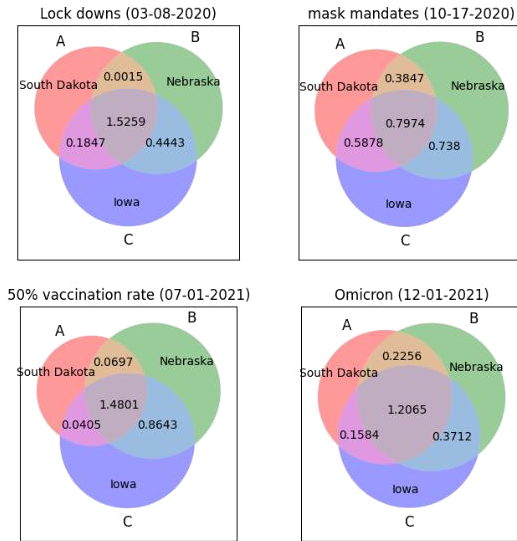


Fig. 8. 4 Venn diagrams of Nebraska, Iowa, South Dakota at different time periods. Note the label Nebraska, Iowa, South Dakota are hiding huge negative MI  $-(1.75 \pm 0.75)$ .

resents the SE of every state, we got the MI using the formula  $I(XY) = H(X) + H(Y) - H(XY)$  (where  $H(X, Y)$  is joint entropy) [7]. MI means the amount of information that the two states shared. For example, South Dakota and Iowa shared  $1.5259 + 0.1847 = 1.7106$  bits of information in this case. From the four figures, we know the  $MI \geq 1$  except "mask mandates", especially the "lockdown" process has the highest shared MI. From the [fig.8], we know the Covid cases among the three states are almost the same during the "lockdown" period. In other words, we can predict the later Covid dynamics of one state by giving the Covid data of other states. Therefore, we know the hypothesis is correct.

### III. DISCUSSION AND CONCLUSIONS

While there were few complications to compute and calculate entities, we were able to extract results using different methods from Walker's paper. To demonstrate the transition, the writer took an example of top-down causation first. This example is about wings, offsprings have what the ancestor doesn't have, which means the offsprings are affected by the environment. Then the writer presented a toy model, investigated the collective behavior in a globally coupled logistic map to show how the information flow from bottom-up and top-down. From the fig.3 on page 5, we can know, as the coupling strength increases, more collective phenomena are found.

From the logistic map, we can know as the  $R$  increases, the system goes to a fixed point, oscillate between two different values, four different values .. until chaotic [8]. This is like Covid dynamics, if the infection rate is pretty low, the number

of infected people will maintain at an exact number, which is predictable. The higher the infection rate is, the harder it is to predict the number of infected people.

Observing the data of Covid cases we can know they are affected by many factors. Just like bottom-up causation, mask mandates, lockdown, or holidays can all influence the data. The changes in data influence those measures vice versa. If data increases, more strict measures will be taken, more vaccinations will be invented. Thus, it's more like top-down causation.

### ACKNOWLEDGMENT

We would like to start out by thanking the authors of the paper "The coupled Logistic Map" Justin Deterding and Catherine Wright for their code and paper. We would also like to thank Mark Eberlein for his non-system-dependent docker of the Deterding and Wright code. We want to give a big thanks to Matthew Timm but not his brother Sean Timm for helping us with the code for fig. 4 & fig. 5. Next we would like to thank our supergroup in no particular order: Eliza Gilber, Wesley Swedenburg, Viacheslav Zhuravlev and Liangkun Yu.

### REFERENCES

- [1] S.I.Walker, L.Cisneros, P.C.W. Davies. "Evolutionary Transitions and Top-Down Causation," Phil. Trans. Artificial Life 13, Feb 2012.
- [2] J. Deterding, C. Wright. "The Coupled Logistic Map" 19, Feb 2020.
- [3] M.Moses, "Logistic Map Lecture," 20, Jan 2022.
- [4] M. Mitchell, "Complexity: a guided tour," Oxford: Oxford University Press, 2011.
- [5] J.Deterding, C.Wright, "CS523-TopDownCausation," 2020. <https://github.com/judeter/CS523-TopDownCausation>, 2022.
- [6] ovid, "Covid-19-data" 2022. , 2022.
- [7] [https://en.wikipedia.org/wiki/Mutual\\_information](https://en.wikipedia.org/wiki/Mutual_information)
- [8] M. Young, The Technical Writer's Handbook. Mill Valley, CA: University Science, 1989.